Geochemistry Geophysics Geosystems G3
AN ELECTRONIC JOURNAL OF THE EARTH SCIENCES
Published by AGU and the Geochemical Society

Article
Volume 9, Number 3
7 March 2008
Q03006, doi:10.1029/2007GC001925
ISSN: 1525-2027

Composition and structural control of crustal domains in the central Andes

Mirian Mamani
Abteilung Geochemie, Universität Göttingen, Goldschmidtstrasse 1, D-37077 Göttingen, Germany (mmirian@gwdg.de)

Andrés Tassara
Departamento de Geofísica, Universidad de Chile, Blanco Encalada 2002, Santiago, Chile

Gerhard Wörner
Abteilung Geochemie, Universität Göttingen, Goldschmidtstrasse 1, D-37077 Göttingen, Germany

[1] Present-day ratios of Pb isotopes (324 published samples, 435 new) and Nd-Sr isotopes (150 published, 180 new) on Proterozoic to Holocene igneous, metamorphic, and sedimentary rocks define (at high spatial resolution) distinct isotopic domains of the crust in the central Andes. These domains correlate with the internal compositional structure of the crust as revealed by a three-dimensional density model. Pb-Nd isotopic boundaries thus correspond to variations in crustal compositional structure and reflect Proterozoic mafic-dominated and Paleozoic felsic-dominated crustal lithologies. Age and composition (mafic versus felsic) of these domains have controlled the rheology of the Andean crust, have influenced crustal deformation patterns, and correlate with the central Andean plateau segmentation.

Components: 7380 words, 6 figures.

Keywords: central Andes; mafic; felsic; crustal domains; density structure; isotopic composition.

Index Terms: 8104 Tectonophysics: Continental margins: convergent; 1040 Geochemistry: Radiogenic isotope geochemistry; 1219 Geodesy and Gravity: Gravity anomalies and Earth structure (0920, 7205, 7240).

Received 8 December 2007; **Accepted** 26 December 2007; **Published** 7 March 2008.

Mamani, M., A. Tassara, and G. Wörner (2008), Composition and structural control of crustal domains in the central Andes, *Geochem. Geophys. Geosyst.*, *9*, Q03006, doi:10.1029/2007GC001925.

1. Introduction

[2] Various studies have shown that lead isotopic compositions of igneous rocks in the central Andes reflect the composition of the underlying basement and thus can be used to (1) map crustal domains [*Wörner et al.*, 1992; *Aitcheson et al.*, 1995] and (2) constrain plate reconstructions [*Tosdal*, 1996; *Loewy et al.*, 2004]. *Macfarlane et al.* [1990] suggested from Pb isotope data that Andean ore deposits are mixtures of mantle and crustal sources, reflecting distinct geological provinces. In this contribution, we analyze the results of 759 Pb and 230 Nd isotope analyses on metamorphic, intrusive and volcanic rocks ranging in age from Proterozoic to Holocene, for the central Andes (13° to 28°S and 75° to 65°W). This data set identifies present-day crustal domains and locates their boundaries at a high spatial resolution. These results show correlation with the crustal structure

derived from a 3-D density model, indicating that changes of Pb and Nd isotope compositions of igneous and basement rocks are caused by variations in the proportions of light, felsic to dense, mafic material of the crust in the central Andes. Such coherence implies that crustal evolution and structure, major element composition, and trace elements are linked through time and control magma compositions and the structural grain during Andean orogeny.

2. Tectonic Setting

[3] The Andean margin has been shaped by convergence between oceanic plates of Pacific affinity and the western edge of South America since Jurassic times [*Allmendinger et al.*, 1997; *Ramos and Aleman*, 2000]. Currently, the oceanic Nazca plate and the South American plate converge with an azimuth of N79°E and a rate of ~63 mm/a for the central Andean margin [*Kendrick et al.*, 2003]. This convergence direction is roughly parallel to the axis of symmetry of the margin at ~20°S, defined by *Gephart* [1994] in terms of surface topography and slab geometry.

[4] The Peru-Chile trench has a maximum depth of 8000 m. It is almost free of sediments and no accretionary prism is observed along the central Andean margin [*von Huene et al.*, 1999]. Eastward of the coastline, uplifted metamorphic rocks of Proterozoic and Paleozoic age and intermediate-to-basic Jurassic-Cretaceous magmatic rocks are exposed along the Coastal Cordillera. Subaerial forearc basins are filled with Cenozoic volcano-sedimentary deposits of the Moquegua Group and Azapa Formation [*Roperch et al.*, 2006; *Wörner et al.*, 2000b]. The Western Cordillera (max. elevations 6000 m) is a chain of Quaternary stratovolcanic complexes (Figure 3a; see Geomorphological Units). This geomorphological unit also contains exposures of well-preserved volcanic structures of middle Miocene to Pliocene ages. The Altiplano (14–21°S) is an internally drained basin filled with gently deformed Cenozoic synorogenic sediments and volcanics [*Allmendinger et al.*, 1997] with an average elevation of 3800 m [*Isacks*, 1988]. The Puna (22–27°S) has an average elevation nearly a kilometer higher than the Altiplano, which has been attributed to thermal uplift caused by thinning of the lithosphere and delamination beneath the Puna [*Whitman et al.*, 1996]. Thinned crust and lithosphere beneath the Puna plateau have also been suggested on the basis of the chemistry and isotopic composition of back-arc volcanics [*Kay et al.*, 1994]. The eastern boundary of the Altiplano-Puna Plateau is the Eastern Cordillera (max. elevations 5000 m), a doubly vergent deformation belt active until the middle to late Miocene [*McQuarrie*, 2002]. Present-day crustal shortening concentrates along the Sierras Subandinas fold-thrust belt [*Kley et al.*, 1999].

[5] *Ramos* [1988] and *Ramos and Aleman* [2000] defined the nature and regional distribution of various terranes in the Andean belt on the basis of tectonostratigraphic analysis (Figure 1). These terranes form a mosaic of old continental crust amalgamated during the Late Proterozoic to early Paleozoic times [*Tosdal*, 1996; *Loewy et al.*, 2004, and references therein] and a noncollisional Paleozoic mobile belt at the western edge of Gondwana [*Lucassen et al.*, 2001; *Lucassen and Franz*, 2005; *Chew et al.*, 2007]. Crucial for our reconstruction of the terrane assemblage of the central Andes is the Proterozoic Arequipa terrane. This is formed by discontinuous outcrops of mafic Proterozoic basement rocks exposed in the Peruvian Coastal Cordillera, in the western Altiplano and along the Chilean Precordillera to the north of 22°S [e.g., *Tosdal*, 1996; *Wörner et al.*, 2000a; *Loewy et al.*, 2004].

3. Analytical Techniques

[6] Major, trace elements, and strontium, neodymium and lead isotopes of the samples were measured on whole-rock by X-ray fluorescence analysis (XRF) and thermal ionization mass spectrometry (TIMS) at the ''Geowissenschaftliche Zentrum'' of the University of Göttingen.

[7] For XRF 700 mg of powdered sample were thoroughly mixed with 4200 mg Spectroflux 100 (Dilithiumtetraborate [$Li_2B_4O_7$]) and melted to a glass disc by an automatic fusion device. Analytical errors for major elements are around 1% (except for Fe and Na, 2%) and for trace elements around 5%. For the calibration of major and trace element determination were used about 50 reference materials: a wide variety of international geochemical reference samples from the US Geological Survey, the International Working Group ''Analytical standards of minerals, ores and rocks'', the National Research Council of Canada, the Geological Survey of Japan, the South African Bureau of Standards, the National Institute of Standards and Technology.

[8] The isotope ratios of Sr, Nd and Pb on whole rocks were determined by TIMS (Finnigan MAT262-RPQII). For Sr and Nd isotopic determi-

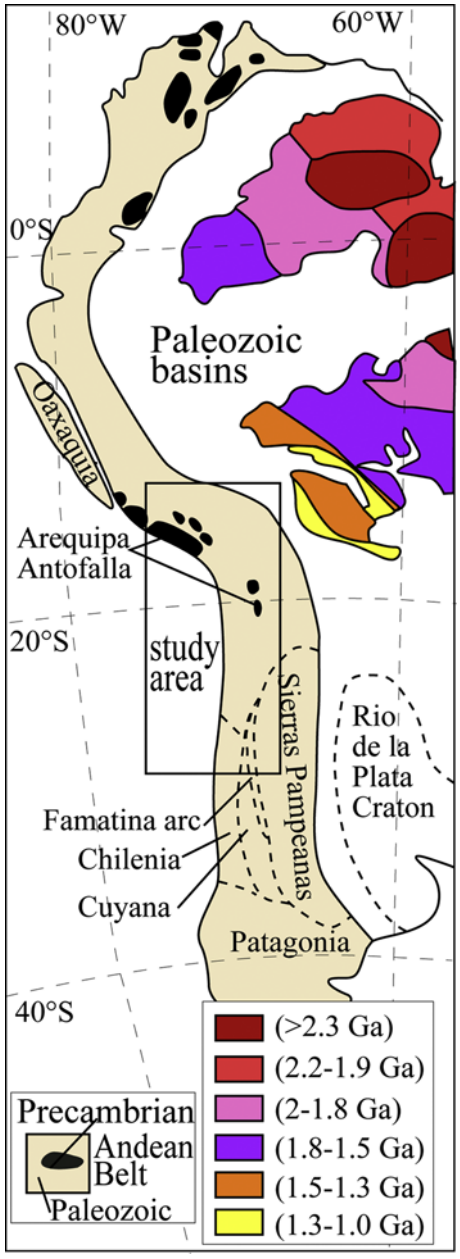

Figure 1. Map of the western South America margin illustrating the major tectonic provinces and the ages of their most recent metamorphic overprints (adapted from *Chew et al.* [2007] and *Ramos and Aleman* [2000]).

nation 100 mg of sample powder was dissolved in 6 mL HF: HNO3 (1:1) for 16 hours at 200°C baked within Savillex beakers. The solution was evaporated to complete dryness at 140°C on a hot plate, dissolved and evaporated two times again in 4 mL 6 N HCl, and evaporation for the last time, it was redissolved in 2.5 mL 2.6 N HCl, stored in PE vials and centrifuged. For separation the sample solution was rinsed with 2.6 N HCl through columns containing ion exchange resin BIORAD AG 50W-X8 Resin, 200–400 mesh. The strontium-rich elution fraction was collected and evaporated to dryness and stored until measuring. For Nd separation, the REE rich fraction gained from the above separation sequence was separated in a second set of columns containing Teflon powder which is impregnated with ion-exchanging HDEHP Bis-(2-etylhexy)-Phosphate. Elution of Nd was done with 0.18 N HCl. For measurement, Sr was dissolved in 0.5 N H_3PO_4 and mounted on Re-double filaments (~1 μg), and Nd was dissolved in 2 N HCl and mounted on Re-double filaments (~1 μg). The Sr and Nd isotope ratios were corrected for mass fractionation to $^{87}Sr/^{86}Sr = 0.1194$ and $^{143}Nd/^{144}Nd = 0.7219$ and normalized to values for NBS987 (0.710245), and La Jolla (0.511847), respectively. Measured values of these standards over the period of the study were 0.710262 ± 24 (21 analyses) and 0.511847 ± 20 (12 analysis). External 2σ errors are estimated at <0.004% for Sr and Nd. Total procedural blanks are: Sr (0.26 ng) and Nd (<0.14 ng). For Pb isotopic determination about 100 mg of sample powder was dissolved in 4 mL HF: HNO_3 (1:1) in Savilex beakers at 200°C for 24 hours. After dilution in 1 mL 0.5 N HBr and subsequent evaporation, it was diluted again in 0.5 N HBr and centrifuged. Lead was separated on anion exchange columns containing 100 μl resin (Biorad AG1-X8, 200–400 mesh). The samples were dissolved in 0.3 mL 2 N HCl and washed into the columns, then with 1 ml 0.5 N HBr and finally eluted with 1 mL 6 N HCl. To get rid of alkalis and alkali earths, the separation process was repeated. The entire process was carried out in a laminar flow box to exclude contamination by lead which is bound to dust particles. Pb was mounted on Re double filament using silica-gel. Lead isotopes were corrected to NBS 981. Normalization of our data to recommended values was performed using a mass fractionation factor of 0.122%. Twenty one standard measurements gave means of $^{206}Pb/^{204}Pb = 16.90 \pm 0.01$, $^{207}Pb/^{204}Pb = 15.44 \pm 0.02$, $^{208}Pb/^{204}Pb = 37.53 \pm 0.05$, total error (2$\sigma$) < 0.1% were determined. Total blank were 0.29 ng. Ionization temperature for Pb measurement was held constant at 1200°C and controlled by an optical temperature-reader.

4. Pb Isotope Domains

[9] Isotope data for metamorphic basement rocks of the central Andes are rare and come only from a few scattered outcrops of the Proterozoic Arequipa basement of southern Peru, northern Chile and western Bolivia (20 samples from *Bock et al.*

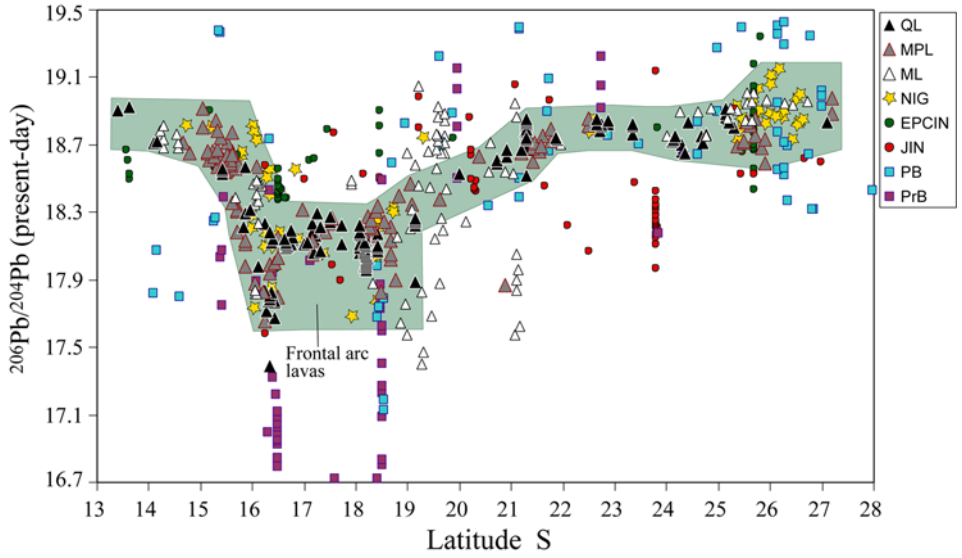

Figure 2. The $^{206}Pb/^{204}Pb$ ratios as a function of latitude in the central Andes. Quaternary lavas (QL), Mio-Pliocene lavas (MPL), Miocene lavas (ML), Neogene ignimbrites (NIG), Eocene-Paleocene-Cretaceous intrusions (EPCIN), Jurassic intrusions (JIN), Paleozoic basement (PB), and Proterozoic basement (PrB). The shaded field highlights the lead isotope ratios of Miocene to Recent frontal arc lavas. Equivalent diagrams for $^{207}Pb/^{204}Pb$ and $^{208}Pb/^{204}Pb$ are given in the auxiliary material; see text for discussion.

[2000] and *Loewy et al.* [2004] and 11 new samples). Paleozoic basement rocks of the Eastern Cordillera, across the Western Cordillera and Altiplano-Puna have a lower metamorphic grade (71 samples from *Lucassen et al.* [2001, and references therein] and *Kamenov et al.* [2002] and 16 new samples). Igneous Jurassic rocks have been analyzed from the Coastal Cordillera (52 samples from *Lucassen et al.* [2006, and references therein] and 14 new samples). These and 50 published [*Rogers and Hawkesworth*, 1989; *Haschke et al.*, 2002] and 8 new data on Cretaceous igneous rocks were combined with 522 Pb isotope ratios of Cenozoic igneous rocks (136 samples from *Kay et al.* [1999, and references therein], *Trumbull et al.* [1999], *Siebel et al.* [2001], and *Aitcheson et al.* [1995] and 386 new data). The new database and the compilation of the published data are available as auxiliary material[1] (Tables S1 and S2).

[10] This large number of Pb isotope measurements of Andean rocks (i.e., gneisses, intrusions, ignimbrites, and lavas), ranging in age from Proterozoic to Recent (Figure 2) allows to outline the crustal domains (Figure 3a) much more precisely than previously possible. We include data from rocks of very different ages. Even though their paleogeographic arrangement was different in Proterozoic, Paleozoic and Neogene times, we argue that the crustal column (with the exception of the sub-Andean belts) largely remained unchanged unless significant differential movements occurred between upper and lower crust, which is beyond the resolution of the domain boundaries outlined below. In this case, a Mesozoic or Tertiary magmatic rock will be within the geological and geographical context of the Proterozoic crustal domain into/onto which it was emplaced. If younger volcanic rocks traverse (and assimilate) this crust, they again will represent this domain. However, in more recent geological times (i.e.,<15 Ma) lower crustal flow must be considered. Lower crustal flow from E to W was invoked to explain uplift of >2000 m of the western margin of the Altiplano that occurred with only limited shortening [*Sempere and Jacay*, 2007; *Hindle et al.*, 2005; *Wörner et al.*, 1992; *Isacks*, 1988]. Lower crustal flow would cause the E boundary of the Arequipa Domain (see discussion below) to be more diffuse and shift its western boundary to the W toward the Coastal Cordillera. If the spatial resolution of our domain boundaries is near the distance of lower crustal flow, then this process will have relatively little affect on their location. It is therefore justified

[1]Auxiliary materials are available in the HTML. doi:10.1029/GC001925.

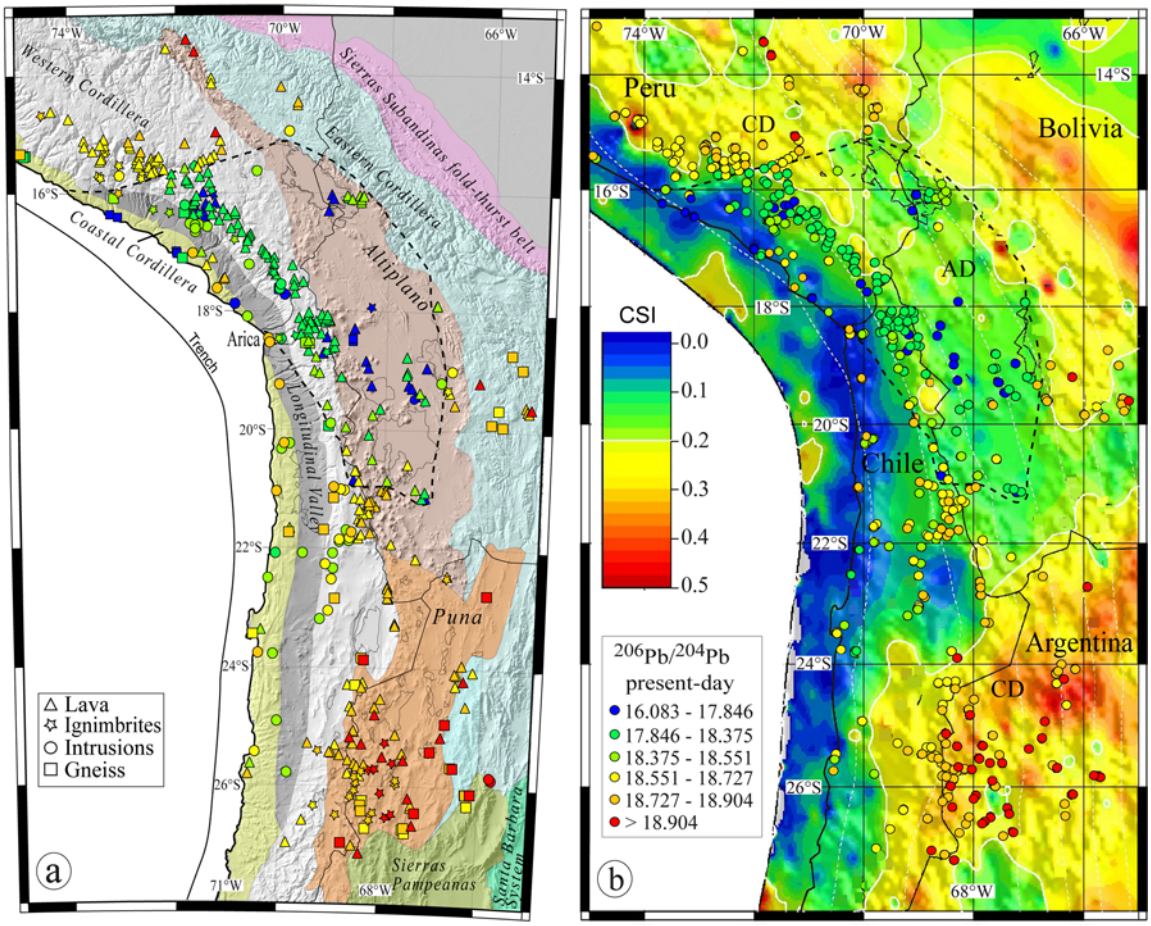

Figure 3. (a) Spatial distribution of Pb isotope ratios in the central Andes (compositions of Proterozoic and Meso-Cenozoic igneous and metamorphic rocks (color code for $^{206}Pb/^{204}Pb$ values in Figure 3b)). Map also shows principal geomorphological units. (b) Map of the "crustal structure index CSI" for the central Andes and compared to Pb isotope values. AD, Arequipa domain; CD, Cordillera domain. Dashed black line is the approximate contour of the Arequipa domain. Dashed black lines are depth contours of the subducting slab at 100 km.

to "mix" old and young rocks in our analysis. On this basis, we distinguish the following domains:

[11] The Arequipa domain is represented by the lowest $^{206}Pb/^{204}Pb$ ratios (from 16.083 to 18.551), $^{207}Pb/^{204}Pb$ ratios (15.435 to 15.650) and $^{208}Pb/^{204}Pb$ ratios (37.625 to 38.655). The Neogene volcanics in this domain have lower ε_{Nd} values from −4 to −12 (Figures 4 and 5c) and high $^{87}Sr/^{86}Sr$ ratios from 0.706 to 0.708 (Figure 5d). The northern boundary (~16°S) of this domain is abrupt compared with the southern boundary (between 19.3°S and 21°S).

[12] The Cordillera domains occur to the S and N of the Arequipa domain and have the highest Pb isotope ratios: $^{206}Pb/^{204}Pb > 18.551$, $^{207}Pb/^{204}Pb > 15.650$, and $^{208}Pb/^{204}Pb > 38.655$. Neogene volcanoes in the northern Cordillera domain have low ε_{Nd} from −1 to −4 (Figures 4 and 5c), low $^{87}Sr/^{86}Sr$ ratios from 0.705 to 0.7064 (Figure 5d). The southern Cordillera Domain has ε_{Nd} from −2 to −8 (Figures 4 and 5c) and $^{87}Sr/^{86}Sr$ ratios from 0.705 to 0.708 (Figure 5d).

[13] Mesozoic rocks along the Coastal Cordillera have $^{206}Pb/^{204}Pb = 18$ to 19. These isotopes ratios are generally higher than that of the Proterozoic basement ($^{206}Pb/^{204}Pb = 16.7$ to 18.4) on which they are located. However, $^{207}Pb/^{204}Pb$, $^{208}Pb/^{204}Pb$ and in some cases $^{206}Pb/^{204}Pb$ (e.g., between 22°S–27°S, at 18°S and 20.2°S) are similar to the basement where they are located. Their higher ε_{Nd} values (5 to −1, Figure 4) and low $^{87}Sr/^{86}Sr$ ratios (0.703 to 0.705) are relatively close to mantle values and thus representative of a

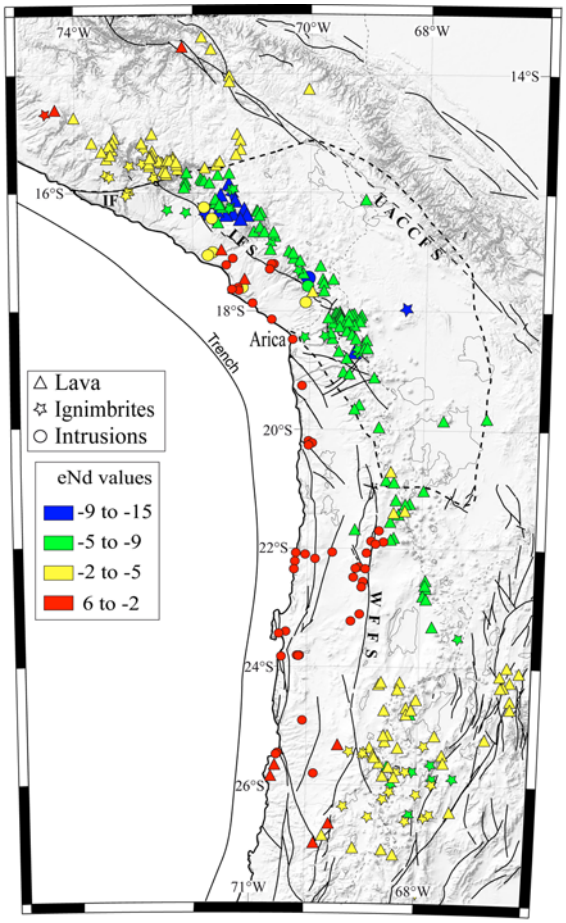

Figure 4. Regional variation of eNd values. The boundary of the Arequipa Domain as defined in Figure 3 is outlined by dashed line. Black lines are the principal fault systems. Urcos-Ayaviri-Copacabana-Coniri fault system (UACCFS), Incapuquio fault system (IFS), West fissure fault system (WFFS) and Iquipi fault (IF).

largely juvenile magma addition to the crust in Jurassic and Cretaceous times [*Lucassen et al.*, 2006; *Bock et al.*, 2000].

5. Crustal Structure Index Derived From 3-D Density Modeling

[14] The three-dimensional density model of *Tassara et al.* [2006] was designed to represent the current distribution of mass along the Andean margin (5°S–45°S) at continental scales. The structure of the model is formed by a number of bodies simulating the subducted slab, the subcontinental mantle and the continental crust. Each body has one value of density, which is appropriated for its expected chemical composition, metamorphic pressure-temperature conditions, water content and degree of partial melting. The geometries of the slab, lithosphere-asthenosphere boundary, and continental Moho were prefixed, as far as available geophysical data allow (for location and sources of data, see *Tassara et al.* [2006]). Because the geophysical database for the central Andes constrains the subcrustal slab geometry very well, the geometry of the intracrustal density distribution remains as the unique degree of freedom during the forward modeling of the Bouguer anomaly. This intracrustal density discontinuity (ICD) is the boundary between an upper-crustal body with a density of 2.7 g/cm^3 and a lower-crustal body with density 3.1 g/cm^3. Following empirical relationships between density, silica content and hydration degree of crystalline crustal rocks [*Tassara*, 2006], the upper-crustal body simulates a granitic upper crust with ~70 wt% SiO_2, whereas the dense lower-crustal body represents a garnet-pyroxene dry granulite of 55–58 wt% SiO_2 or a more basic but hydrated amphibolite with 55–48 wt% SiO_2.

[15] The geometry of the ICD is a proxy to regional-scale (several tens to a few hundred kilometers) lateral density variations within the crust produced by variations in the bulk compositional structure of the crust, i.e., the vertically integrated proportion of felsic to mafic crust. On the basis of the geometries of the 3-D density model of *Tassara et al.* [2006], we computed the "crustal structure index (CSI)" for the study area as the ratio between the thicknesses of the lower-density upper-crustal body and the total crustal thickness. Low or high values of CSI indicate a predominance of mafic or, respectively, felsic material in the crust (Figure 3b).

6. Correlations Between Geochemical Domains and Crustal Density Structure

[16] Variations in "crustal structure index CSI" along the central Andes strongly correlate with isotope domains (Figure 3b). Low CSI (<0.2) coincides with the unradiogenic Arequipa and Coastal domains. High CSI values (>0.2) correlate with the Cordillera Domains.

[17] These observed CSI geometry, combined with correlated isotope domains, indicate that significantly higher CSI values are found for relatively more felsic Andean basement, which are located toward the north and south of the more mafic Arequipa basement with low CSI.

[18] Such a correlation between 3-D density structure and Pb domains then also indicates that the

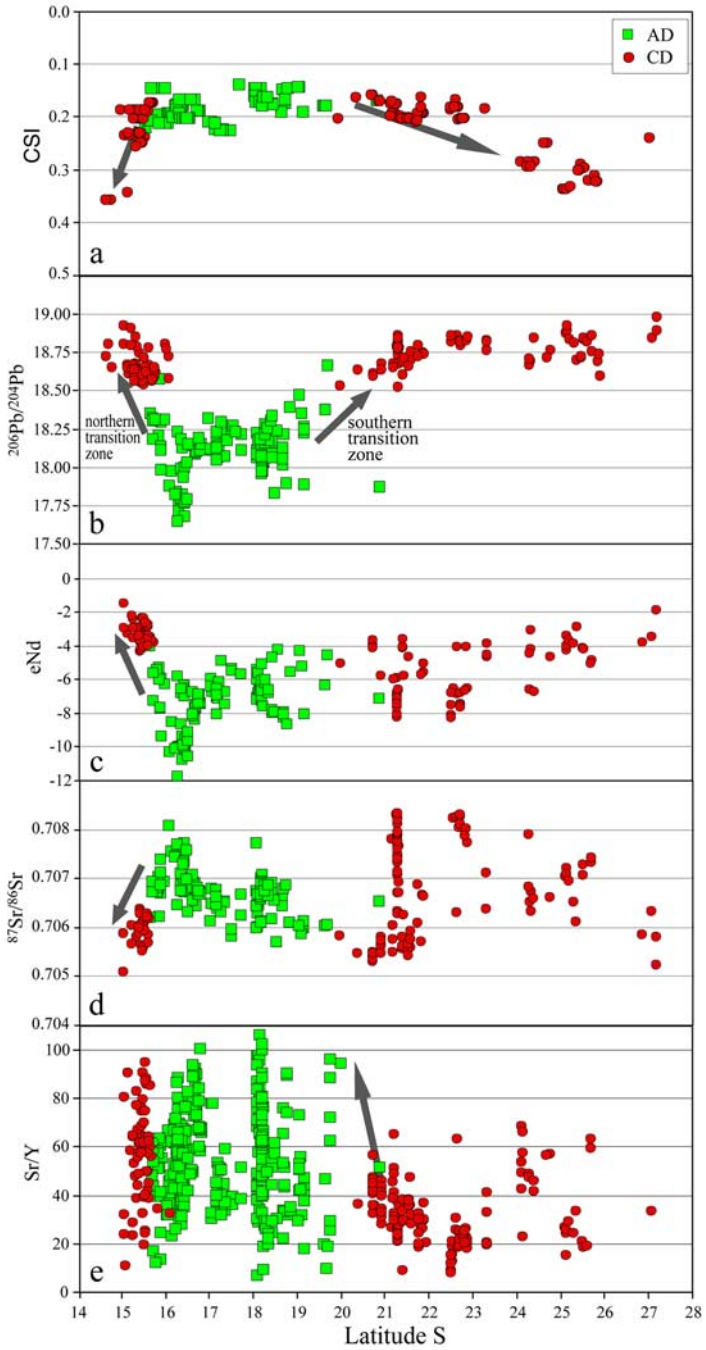

Figure 5. Variations in $^{206}Pb/^{204}Pb$ isotope ratios, eNd values, $^{87}Sr/^{86}Sr$ isotope ratios, and Sr/Y ratios in lavas <10 Ma old along the frontal arc. AD, Arequipa domain; CD, Cordillera domain. Arrows highlight variations of geochemical and geophysical data.

proportion between felsic and mafic crust are the main factors controlling the density structure as well as isotopic and geochemical variations of the central Andean crust. With age, the compositional differences will translate into enhanced isotopic differences.

[19] Nd values further support our crustal domain distinctions and corroborate the domain boundaries defined here on the basis of Pb isotopes (Figure 4). In some areas (e.g., to the southern boundary of Arequipa domain, Figure 5d) Sr isotope variations do not constrain the boundaries of crustal domains

very well. This is because the domain boundary may be cutting the crust at a shallow angle and thus assimilation and mixing from different domains at different depths will cause a transition rather than a sharp boundary (Figure 5b) [*Wörner et al.*, 1992]. Also Sr isotopic compositions are much less distinctive in the crust from different domains.

[20] By contrast, the northern boundary of the Arequipa domain is very well constrained also by Sr isotopes (Figure 5d) and this suggests that the northern edge of Arequipa terrane is relatively abrupt and steep. The crustal density structure (Figures 3b and 5a) at this boundary also changes abruptly, unlike the southern boundary (between 21°S and 22°S) where the transition between mafic and felsic is wide (Figures 3, 5a, and 5b).

[21] Major juvenile additions to the crust are located along the Coastal Cordillera. Here, the Jurassic and Cretaceous igneous rocks have isotopic compositions close to mantle sources [*Lucassen et al.*, 2006] and the crust seems to be mostly mafic (CSI < 0.1).

7. Geochemical Signatures and Isotopic Crustal Domains

[22] Upper and lower crust will likely have similar age and tectonic history within the resolution of the domain boundaries (~50 km) unless large scale lateral differential movements occurred recently between upper and lower crust. However, similar ages and similar evolution with a crustal column does not necessarily imply that upper and lower crust must be of the same composition. Therefore, the very sparse surface outcrops of basement will not be fully representative of the lower crust of the central Andes and even if sparse examples of upper crustal rocks tend to be relatively silicic [*Cobbing et al.*, 1977; *Shackleton et al.*, 1979; *Wasteneys et al.*, 1995; *Tosdal*, 1996], the lower crust could still be largely and relatively more mafic. Therefore, the analysis of igneous rocks that traverse the Andean crust may well be a better "probe" to the composition of the bulk crust than sparse outcrops.

[23] As we argue here, a larger portion of the crust in the Arequipa domain tends to be more mafic. However, at least toward the N, the supposedly less mafic crust is lower in Sr and higher in Nd isotopes (Figures 5c and 5d). This apparent contradiction could have the following explanation: The isotopic composition of basement rocks will be the result of the combination of composition and age. If "depleted" mafic lower crust is very old, it still can, for example, grow in more radiogenic Sr than a younger, more silicic crust. Moreover, the effect on the isotopic composition of the younger volcanic rocks, which "probe" the crust through assimilation will be different for different isotopic systems. Pb will be easily overwhelmed by the crustal signature even at low degrees of assimilation, whereas Sr and Nd isotopes will not only be dependant on the isotopic composition of the assimilant but also on the amount of assimilation. Sr and Nd isotope signatures thus could be partly and variably decoupled from each other and from the nature of the crust (mafic versus silicic). By contrast, Pb isotopes should represent the most reliable crustal signature. Therefore, the isotopic signature of "mafic" crust as represented by magmatic rocks that have traversed this crust, does not necessarily imply that Sr must be less radiogenic and Nd more radiogenic.

[24] Another argument with respect to the mafic/silic composition of the crust comes from trace element variations in Neogene volcanic rocks. It has been proposed [e.g., *Kay et al.*, 1999; *Haschke et al.*, 2002] that high Sr/Y in magmas traversing thickened crust in the central Andes implies a role of garnet in magma genesis, either in a high-pressure mineral assemblage in the crustal residue after assimilation or as a fractionating phase. However, the stability of garnet in crustal rocks does not only increases with pressure (i.e., depth) but it also decreases with increasing silica content in the crustal reservoir [*Sobolev and Babeyko*, 1994; *Tassara*, 2006]. Figure 5e shows that the highest Sr/Y ratios of young volcanoes (<6 Ma) occur in the Arequipa domain, i.e., between 16°S and 20°S, in spite of the fact that the crust below the central Andes has everywhere a thickness >65 km [*Tassara et al.*, 2006]. Low Sr/Y even on thick crust would imply either felsic bulk crustal composition, as could be the case of volcanoes on the southern Cordillera domain, or assimilation occurred mostly in the upper crust as can be inferred for some volcanoes with low Sr/Y ratios on the Arequipa domain.

[25] The $^{206}Pb/^{204}Pb$ ratios show the largest absolute variations and have thus been used here to outline the domain boundaries. However, the same general pattern is shown for $^{207}Pb/^{204}Pb$ and $^{208}Pb/^{204}Pb$ ratios (auxiliary material Figures S1 and S2). These diagrams and maps also show that wherever "extreme" low values in crustal rocks (gneisses, granulites) occur, the spatially associated

volcanic rocks also show "excursions" from the general pattern (e.g., $^{206}Pb/^{204}Pb$ at 16.5°S, Figure 2). $^{207}Pb/^{204}Pb$ would be expected to show less variability due to the faster decay rates of ^{235}U to ^{207}Pb if the U/Pb fractionation process in the crust occurred within the last 1 to 2 Ga. This is in accord with the known crustal formation and metamorphic ages of the Central Andean Basement [*Loewy et al.*, 2004; *Tosdal*, 1996; and references therein]. Comparing $^{207}Pb/^{204}Pb$ and $^{208}Pb/^{204}Pb$ with $^{206}Pb/^{204}Pb$ regional trends (Figure 2 and auxiliary material Figures S1 and S2) shows that in detail there is a finer-scale pattern to the data: The lowest $^{206}Pb/^{204}Pb$ ratios (17.62 to 18.20), lowest $^{207}Pb/^{204}Pb$ ratios (15.52 to 15.63) and higher $^{208}Pb/^{204}Pb$ ratios (38.30 to 38.75) are between 15°S and 17°S, contrarily between 17.5°S and 19°S lavas have higher $^{206}Pb/^{204}Pb$ ratios (17.8 to 18.3), $^{207}Pb/^{204}Pb$ ratios (15.57 to 15.65) and low $^{208}Pb/^{204}Pb$ ratios (37.77 to 38.70). This indicates the existence of "subdomains" in the Arequipa Domain with different ages and U/Pb and Th/Pb fractionation histories [see also *Loewy et al.*, 2004].

8. Compositional and Structural Segmentation of the Central Andean Crust

[26] The northern boundary between the Arequipa domain and the northern Cordillera domain should be relative sharp within the crust, because sample sites close to each other systematically show very different isotopic compositions and the CSI changes quite markedly along this boundary. Therefore the northern boundary of Arequipa domain would follow a deep E–W structure, which exactly coincides with a crustal reverse fault recognized at the surface as the Iquipi fault (Figure 4) [see *Roperch et al.*, 2006]. This is in contrast with the southern boundary of the Arequipa domain that seems to be more diffuse both in terms of Pb isotopic composition and CSI geometry [*Wörner et al.*, 1992].

[27] *Schmitz et al.* [1997] and *Yuan et al.* [2002] showed that the Moho depth changes at 21°S to 22°S (southern boundary of Arequipa domain) from 70 km in the N to 60 km in the S without a significant change in the Bouguer anomaly. On the basis of this observation they suggest that the crust in the region N of 21°S contains a relatively thicker portion of mafic lower crust. Other studies (e.g., *Lucassen et al.* [2001], *Lucassen and Franz* [2005], and discussion below) confirm that the lower crust below the Puna region is rather felsic-dominated than mafic-dominated.

[28] A striking feature of the central Andean plateau (i.e., Altiplano and Puna) is thus the along-strike variation in topography and tectonic styles [*Whitman et al.*, 1996]. The Altiplano is essentially an internally drained, intermontane basin between the Western and Eastern Cordilleras. In contrast, the Puna is characterized by smaller and more fragmented basins and greater relief. This along-strike change in the plateau topography is also reflected in the different elevation distributions of the two segments: Altiplano elevations are concentrated near 3.8 km while in the Puna elevations are more evenly distributed about a mean elevation of 4.4 km, reflecting the greater local relief [*Isacks*, 1988] and contrasting tectonic histories of the respective segments since the Late Oligocene [*Sempere et al.*, 1990]. The Altiplano also differs from the Puna in the fact that it has a well developed thin-skinned thrust belt to the east which is absent in the Puna foreland [*Allmendinger et al.*, 1997]. North of 23°S, compressional deformation on the Altiplano plateau and in the Eastern Cordillera ceased by 9 Ma, and the locus of horizontal shortening shifted eastward to the low-elevation Sub-Andean fold-thrust belt [*Allmendinger and Gubbels*, 1996]. South of 23°S, however, compressional deformation on the Puna plateau continued to at least 4 Ma and in some locations even to 2 Ma, before changing to strike-slip kinematics [*Allmendinger and Gubbels*, 1996].

[29] Several authors have discussed the role of inherited pre-Andean crustal structures of the upper plate on the Cenozoic geodynamic evolution, deformation and segmentation of the central Andes plateau [e.g., *Allmendinger and Gubbels*, 1996; *Sempere et al.*, 2002]. *McQuarrie and DeCelles* [2001] suggested that the thick Paleozoic sedimentary sequences forming the axis of the Eastern Cordillera may have localized thin-skinned tectonics during shortening in this particular region. For the Puna Plateau, the thick-skinned tectonics of the Santa Barbara System and Sierras Pampeanas has been proposed to have developed over a thermally thinned continental lithosphere and that this segmentation is controlled by the internal crustal structure and delamination in this segment [*Whitman et al.*, 1996]. Delamination was explained as a consequence of the gravitational removal of dense high-grade mafic metamorphic lower crust. Such a process was also suggested by *Kay et al.* [1994] for the Puna

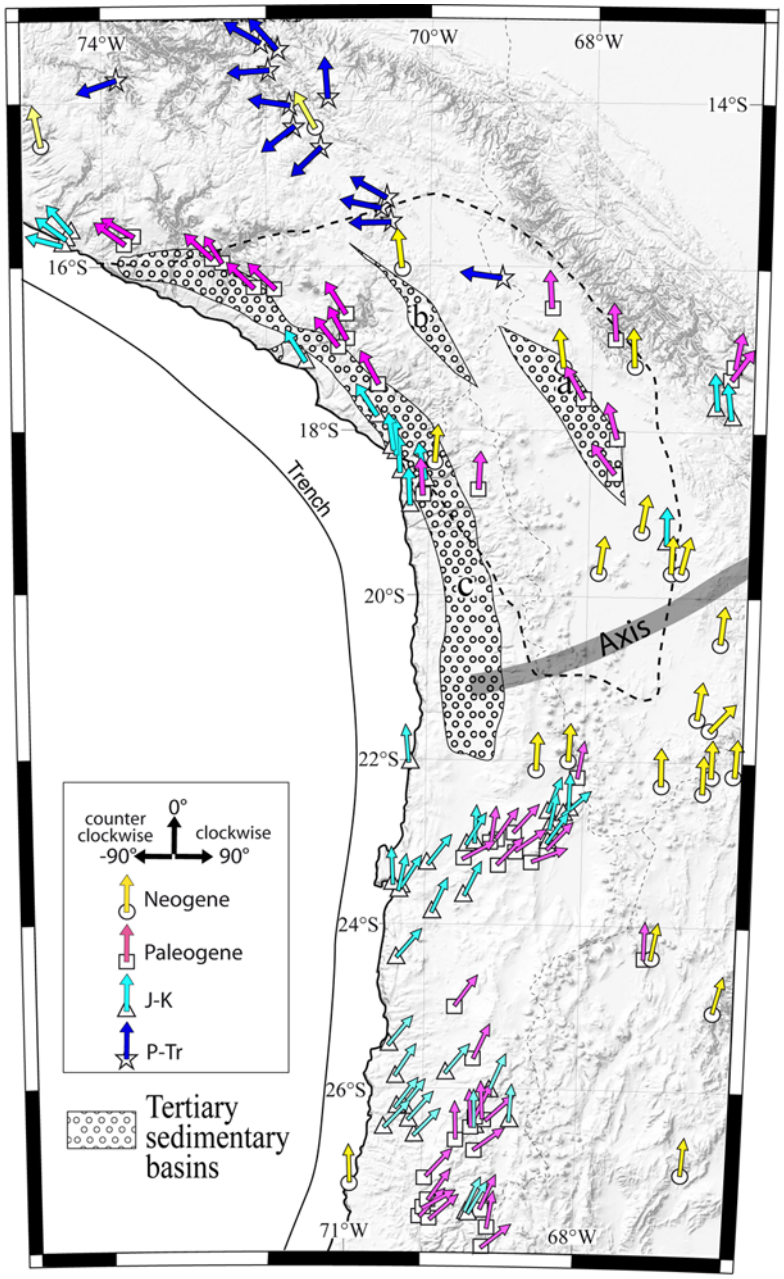

Figure 6. Grey shaded topography (SRTM 1 km) of the central Andes. Dashed black line is the approximate contour of the Arequipa domain as defined in Figure 3. Compilation of tectonic rotations for the central Andes from *Rousse et al.* [2005], *Arriagada et al.* [2006], and *Roperch et al.* [2006]. Sedimentary basins: a, Corque basin; b, Huaccochullo basin; c, Moquegua-Azapa basin. Axis rotation from *Richards et al.* [2004].

plateau to explain timing and occurrence of intraplate mafic volcanism in the area.

[30] The crustal domain boundaries defined here should help to further constrain the role of preexisting crustal heterogeneities in the evolution and deformation pattern of the central Andes. Figure 3a shows that the segmentation of the central Andean plateau and its adjacent foreland is in fact spatially related to the crustal domains defined here: The Arequipa domain is largely coincident with the broad high Altiplano plateau (3.8 km high and 240 km wide). Moreover, the largest amount of shortening in the Eastern Cordillera and sub-Andean belt during Andean Orogeny is located to the E and NE [*Sheffels*, 1990], but is doubtful,

absent or very minor, W and SW of the Arequipa domain [*Sempere and Jacay*, 2007]. The southern boundary of Arequipa domain (between 21°S and 22°S) thus coincides with the transition between the Altiplano and Puna segments. Therefore we argue that the nature, i.e., the bulk composition and thus the different rheologies (i.e., mechanical strength) of the lithosphere and crust are an important factor in controlling the deformation pattern of the central Andes and the localization of the Andean plateau.

[31] Crustal architecture and evolution are also different with respect to Neogene sedimentation patterns with respect to the Arequipa domain: Neogene erosion products deposited during uplift of the central Andes (e.g., Moquegua Group and Azapa Formations and equivalents (Figure 6) [e.g., *Roperch et al.*, 2006; *Wörner et al.*, 2000b]) appear to be much thicker on the forearc of the Arequipa domain.

[32] We will now discuss Andean deformation patterns based on paleomagnetic data. *Arriagada et al.* [2006] described block vertical-axis rotations (clockwise up to 35° to 40°) in the forearc between 22°S and 28°S during the Jurassic to Oligocene, yet the area of rotation and their boundaries are all outside the Arequipa domain (Figures 3b and 6). More to the north in southern Peru, *Roperch et al.* [2006] presented paleomagnetic results from Eocene-Oligocene (~35–25 Ma) sediments from the forearc between 18.3°S and 16°S and observed a gradient in counterclockwise rotations, between ~0° in Arica (18.3°S) to 50° in Caravelí (16°S). These rotations are coeval with, of similar magnitude, but in the opposite sense of the clockwise block rotations in the forearc between 22° and 28°S [*Arriagada et al.*, 2006]. However, on the Altiplano, i.e., on the Arequipa Domain, the Tertiary Huaccochullo and Corque basins (Figure 6) are deformed and rotated counterclockwise as a more or less coherent region [*Rousse et al.*, 2005]. The central Andean rotation pattern as described by *Rousse et al.* [2005], *Arriagada et al.* [2006] and *Roperch et al.* [2006] in fact seems to be related to individual crustal blocks with increased deformation and shear near their margins. Only since Neogene times, the entire central Andes moved coherently (Figure 6) and the structural identity of the earlier blocks is lost.

[33] The Altiplano and its western margin has suffered only limited deformation since about 10 Ma [*Oncken et al.*, 2006, and references therein; *Sempere and Jacay*, 2007], while deformations to the N, S and E continued to more recent times. While the Altiplano and Arequipa domain has been largely undeformed since Miocene times, the deformation pattern of Tertiary differential horizontal shortening is focused in the eastern boundary of the Arequipa domain (Eastern Cordillera) and in the southern Cordillera domain (Puna plateau). The Eastern Cordillera reaches its highest elevations and steepest gradient toward the Altiplano just were it interacts with the eastern margin of the Arequipa Domain.

[34] Moreover, *Richards et al.* [2004] defined a vertical axis rotation (Figure 6) of the Central Andean Orocline on the basis of Euler pole analysis of along strike variations in crustal shortening since 35 Ma and 10 Ma. This axis rotation appears to coincide with the southern boundary of the Arequipa domain.

[35] We conclude from these observations that the mafic Arequipa Domain reacts as a somewhat coherent and rigid block while more diffuse deformation with large vertical axis rotations and faulting are located outside of it. Therefore, the rheological (i.e., mechanical strength) and structural identity of the Arequipa Domain appears to have played an important role during Andean Orogeny.

9. Conclusions

[36] Crustal domains for the central Andes have been identified here on the basis of geochemical and geophysical data. These are interpreted as distinct basement domains of different ages and compositions. Of particular interest is the Arequipa Domain, for which we found evidence that it may have an overall more mafic (higher density) composition. Higher Sr/Y ratios in magmas that traverse the Arequipa Domain (compared to the surrounding Cordillera Domain) could be the result from a garnet-bearing in residual mineralogy in a relatively mafic lower crust. Lower Sr/Y ratios, which are found mostly (but not exclusively) in the Cordillera Domain may imply a minor role for garnet and thus a more felsic crust (or shallower assimilation in the Arequipa Domain) even though the crust has similar thicknesses (>65 km). The interpretation of the Arequipa Domain as a relatively more mafic and possibly more rigid block is tentatively supported by the Cenozoic deformation pattern in the central Andes as well as the distribution and thickness of syn-deformational sedimentary deposits. Deformations and axis rotations are mostly concentrated at its boundaries or in the

surrounding Cordillera Domain. The Coastal Cordillera domain is interpreted as a rigid block with major mafic Mesozoic juvenile (i.e., mafic) contribution to the crust.

Acknowledgments

[37] This work was supported by scholarships of the German Academic Exchange Service (DAAD) to M.M. and A.T. and German Science Foundation grant Wo362/18 to G.W. A.T. thanks the further support of the Chilean Bicentennial Program in Science and Technology grant ANILLO ACT-18. We thank G. Hartmann for providing analytical support, B. Hansen for access to the isotope laboratory, and D. Cassard for invaluable help during data processing. We are thankful to H. Götze, who initiated the comparison between geochemical and geophysical data. Suggestions from S. Kay and C. Hawkesworth on a former version of this manuscript are also acknowledged. We would like to thank T. Sempere and anonymous reviewers for critical reviews of earlier versions of this manuscript.

References

Aitcheson, S. J., R. S. Harmon, S. Moorbath, A. Schneider, P. Soler, E. E. Soria, G. Steele, I. Swainbank, and G. Wörner (1995), Pb isotopes define basement domains of the Altiplano, central Andes, *Geology*, *23*, 555–558.

Allmendinger, R. W., and T. Gubbels (1996), Pure and simple shear plateau uplift, Altiplano-Puna, Argentina and Bolivia, *Tectonophysics*, *259*, 1–13.

Allmendinger, R. W., T. E. Jordan, M. S. Kay, and B. L. Isacks (1997), The evolution of the Altiplano-Puna Plateau of the central Andes, *Annu. Rev. Earth Planet. Sci.*, *25*, 139–174.

Arriagada, C., P. Roperch, C. Mpodozis, and R. Fernandez (2006), Paleomagnetism and tectonics of the southern Atacama Desert (25–28°S), northern Chile, *Tectonics*, *25*, TC4001, doi:10.1029/2005TC001923.

Bock, B., H. Bahlburg, G. Wörner, and U. Zimmermann (2000), Tracing crustal evolution in the southern central Andes from Late Precambrian to Permian using Nd and Pb isotopes, *J. Geol.*, *108*, 515–535.

Chew, D., U. Schaltegger, J. Kosler, M. J. Whitehouse, M. Gutjahr, R. A. Spikings, and A. Miskovíc (2007), U-Pb geochronologic evidence for the evolution of the Gondwanan margin of the north-central Andes, *Geol. Soc. Am. Bull.*, *119*, 697–711, doi:10.1130/B26080.1.

Cobbing, E. J., J. M. Ozard, and N. J. Snelling (1977), Reconnaissance geochronology of the crystalline basement rocks of the Coastal Cordillera of southern Peru, *Geol. Soc. Am. Bull.*, *88*, 241–246.

Gephart, J. W. (1994), Topography and subduction geometry in the central Andes: Clues to the mechanics of a non-collisional orogen, *J. Geophys. Res.*, *99*, 12,279–12,288.

Haschke, M., W. Siebel, A. Günther, and E. Scheuber (2002), Repeated crustal thickening and recycling during the Andean orogeny in north Chile (21°–26°S), *J. Geophys. Res.*, *107*(B1), 2019, doi:10.1029/2001JB000328.

Hindle, D., J. Kley, O. Oncken, and S. Sobolev (2005), Crustal balance and crustal flux from shortening estimates in the central Andes, *Earth Planet. Sci. Lett.*, *230*, 113–124.

Isacks, B. L. (1988), Uplift of the central Andean plateau and bending of the Bolivian Orocline, *J. Geophys. Res.*, *93*, 3211–3231.

Kay, M. S., B. Coira, and J. Viramonte (1994), Young mafic back-arc volcanic rocks as indicators of continental lithospheric delamination beneath the Argentine Puna plateau, central Andes, *J. Geophys. Res.*, *99*, 24,323–24,339.

Kay, M. S., C. Mpodozis, and B. Coira (1999), Neogene magmatism, tectonism and mineral deposits of the central Andes (22°–33°S latitude), in *Geology and Ore Deposits of the Central Andes*, *Spec. Publ.*, vol. 7, edited by B. Skinner, pp. 27–59, Soc. of Econ. Geol., Littleton, Colo.

Kamenov, G., A. W. Macfarlane, and L. R. Riciputi (2002), Sources of lead in the San Cristobal, Pulacayo, and Potosi mining districts, Bolivia, and a reevaluation of regional ore lead isotope provinces, *Econ. Geol.*, *97*, 573–592.

Kendrick, E., M. Bevis, R. Smalley, B. Brooks, R. Barriga, E. Lauría, and L. Souto (2003), The Nazca–South America Euler vector and its rate of change, *J. S. Am. Earth Sci.*, *16*, 125–131.

Kley, J., C. R. Monaldi, and J. A. Salfity (1999), Along-strike segmentation of the Andean foreland: Causes and consequences, *Tectonophysics*, *301*, 75–94.

Loewy, S. L., J. N. Connelly, and I. W. D. Dalziel (2004), An orphaned basement block: The Arequipa-Antofalla basement of the central Andean margin of South America, *Geol. Soc. Am. Bull.*, *116*, 171–187.

Lucassen, F., and G. Franz (2005), The early Paleozoic orogen in the central Andes: A non-collisional orogen comparable to the Cainozoic high plateau?, *Geol. Soc. Spec. Publ.*, *246*, 257–273.

Lucassen, F., R. Becchio, R. Harmon, S. Kasemann, G. Franz, R. Trumbull, H. G. Wilke, R. L. Romer, and P. Dulski (2001), Composition and density model of the continental crust in an active continental margin—The central Andes between 18° and 27°S, *Tectonophysics*, *341*, 195–223.

Lucassen, F., W. Kramer, V. Bartsch, H. Wilke, G. Franz, R. L. Romer, and P. Dulski (2006), Nd, Pb, and Sr isotope composition of juvenile magmatism in the Mesozoic large magmatic province of northern Chile (18–27°S): Indications for a uniform subarc mantle, *Contrib. Miner. Petrol.*, *152*, 571–589.

Macfarlane, A. W., P. Marcet, A. P. LeHuray, and U. Petersen (1990), Lead isotope provinces of the central Andes inferred from ores and crustal rocks, *Econ. Geol.*, *85*, 1857–1880.

McQuarrie, N. (2002), Initial plate geometry, shortening variations, and evolution of the Bolivian orocline, *Geology*, *30*, 867–870.

McQuarrie, N., and P. DeCelles (2001), Geometry and structural evolution of the central Andean back thrust belt, Bolivia, *Tectonics*, *20*, 669–692.

Oncken, O., D. Hindle, J. Kley, K. Elger, P. Victor, and K. Schemmann (2006), Deformation of the central Andean upper plate system—Facts, fiction, and constraints for plateau models, in *The Andes—Active Subduction Orogeny*, *Frontiers in Earth Sciences*, edited by O. Oncken et al., pp. 3–28, Springer, Berlin.

Ramos, V. A. (1988), Late Proterozoic-Early Paleozoic of South America—A collisional history, *Episodes*, *11*, 168–174.

Ramos, V. A., and A. Aleman (2000), Tectonic evolution of the Andes, in *Tectonic Evolution of South America*, edited by U. J. Cordanni et al., pp. 635–685, Int. Geol. Congr., Río de Janeiro, Brazil.

Richards, D. R., R. F. Butler, and T. Sempere (2004), Vertical-axis rotations determined from paleomagnetism of Mesozoic and Cenozoic strata of the Bolivian Andes, *J. Geophys. Res.*, *109*, B07104, doi:10.1029/2004JB002977.

Rogers, G., and C. J. Hawkesworth (1989), A geochemical traverse across the north Chilean Andes: Evidence for crustal generation from the mantle wedge, *Earth Planet. Sci. Lett.*, *91*, 271–285.

Roperch, P., T. Sempere, O. Macedo, C. Arriagada, M. Fornari, C. Tapia, M. García, and C. Laj (2006), Counterclockwise rotation of late Eocene–Oligocene fore-arc deposits in southern Peru and its significance for oroclinal bending in the central Andes, *Tectonics*, *25*, TC3010, doi:10.1029/2005TC001882.

Rousse, S., S. Gilder, M. Fornari, and T. Sempere (2005), Insight into the Neogene tectonic history of the northern Bolivian Orocline from new paleomagnetic and geochronologic data, *Tectonics*, *24*, TC6007, doi:10.1029/2004TC001760.

Schmitz, M. A., W. D. Heinsohn, and F. R. Schilling (1997), Seismic, gravity and petrological evidence for partial melt beneath the thickened central Andean crust (21–23°S), *Tectonophysics*, *270*, 313–316.

Sempere, T., and J. Jacay (2007), Synorogenic extensional tectonics in the forearc, arc and southwest Altiplano of southern Peru, *Eos Trans. AGU*, *88*(23), Joint Assemb. Suppl., Abstract U51B-04.

Sempere, T., G. Herail, J. Oller, and M. G. Bonhomme (1990), Late Oligocene-early Miocene major tectonic crisis and related basin in Bolivia, *Geology*, *18*, 946–949.

Sempere, T., G. Carlier, P. Soler, M. Fornari, V. Carlotto, J. Jacay, D. Néraudeau, J. Cárdenas, S. Rosas, and N. Jiménez (2002), Late Permian-Middle Jurassic lithospheric thinning in Peru and Bolivia, and its bearing on Andean-age tectonics, *Tectonophysics*, *345*, 153–181.

Shackleton, R. M., A. C. Ries, M. P. Coward, and P. R. Cobbold (1979), Structure, metamorphism and geochronology of the Arequipa Massif of coastal Peru, *J. Geol. Soc. London*, *136*, 195–214.

Sheffels, B. M. (1990), Lower bound on the amount of crustal shortening in the central Bolivian Andes, *Geology*, *18*, 812–815.

Siebel, W., W. B. W. Schnurr, K. Hahne, B. Kraemer, R. B. Trumbull, P. van den Bogaard, and R. Emmermann (2001), Geochemistry and isotope systematics of small- to medium-volume Neogene-Quaternary ignimbrites in the southern central Andes: Evidence for derivation from andesitic magma sources, *Chem. Geol.*, *171*, 213–237.

Sobolev, S., and A. Babeyko (1994), Modelling of mineralogical composition, density and elastic wave velocities in the unhydrous rocks, *Surv. Geophys.*, *15*, 515–544.

Tassara, A. (2006), Factors controlling the crustal density structure underneath active continental margins with implications for their evolution, *Geochem. Geophys. Geosyst.*, *7*, Q01001, doi:10.1029/2005GC001040.

Tassara, A., H.-J. Götze, S. Schmidt, and R. Hackney (2006), Three-dimensional density model of the Nazca plate and the Andean continental margin, *J. Geophys. Res.*, *111*, B09404, doi:10.1029/2005JB003976.

Tosdal, R. M. (1996), The Amazon-Laurentian connection as viewed from the Middle Proterozoic rocks in the central Andes, western Bolivia and northern Chile, *Tectonics*, *15*, 827–842.

Trumbull, R. B., R. Wittenbrink, K. Hahne, R. Emmermann, W. Büsch, H. Gerstenberger, and W. Siebel (1999), Evidence for Late Miocene to Recent contamination of arc andesites by crustal melts in the Chilean Andes (25°–26°S) and its geodynamic implications, *J. S. Am. Earth Sci.*, *12*, 135–155.

von Huene, R., W. Weinrebe, and F. Heeren (1999), Subduction erosion along the North Chile margin, *Geodynamics*, *27*, 345–358.

Wasteneys, H. A., A. H. Clark, E. Farrar, and R. J. Langridge (1995), Grenvillian granulite-facies metamorphism in the Arequipa Massif, Peru: A Laurentia-Gondwana link, *Earth Planet. Sci. Lett.*, *132*, 63–73.

Whitman, D., B. Isacks, and S. M. Kay (1996), Lithospheric structure and along strike segmentation of the central Andean plateau, 17°S–29°S, *Tectonophysics*, *259*, 29–40.

Wörner, G., S. Moorbath, and R. S. Harmon (1992), Andean Cenozoic volcanics reflect basement isotopic domains, *Geology*, *20*, 1103–1106.

Wörner, G., J. Lezaun, A. Beck, V. Heber, F. Lucassen, E. Zinngrebe, R. Rössling, and H. G. Wilke (2000a), Precambrian and Early Paleozoic evolution of the Andean basement at Belén (northern Chile) and Cerro Uyarani (western Bolivia Altiplano), *J. S. Am. Earth Sci.*, *13*, 717–737.

Wörner, G., K. Hammerschmidt, F. Henjes-Kunst, J. Lezaun, and H. Wilke (2000b), Geochronology (^{40}Ar-^{39}Ar-, K-Ar-, and He-exposure-) ages of Cenozoic magmatic rocks from northern Chile (18°–22°S)—Implications for magmatism and tectonic evolution of the central Andes, *Rev. Geol. Chile*, *27*, 205–240.

Yuan, X., S. Sobolev, and R. Kind (2002), Moho topography in the central Andes and its geodynamic implication, *Earth Planet. Sci. Lett.*, *199*, 389–402.